LBNL-3409E

HAND-HELD UXO DISCRIMINATOR

MM-1667

2009 INTERIM REPORT

Gasperikova, E., Smith, J.T., Kappler, K.N.,

Ratti, A., Morrison, H.F., and Becker, A.

Lawrence Berkeley National Laboratory

1 Cyclotron Road, MS:90R1116

Berkeley, CA 94720

Phone: 510-486-4930

Fax: 510-486-5686

Email: egasperikova@lbl.gov

April 2010

Disclaimer

1. Introduction

With prior funding (UX-1225, MM-0437, and MM-0838), we have successfully designed and built a cart-mounted **B**erkeley **U**XO **D**iscriminator (BUD) and demonstrated its performance at various test sites (e.g., Gasperikova et al., 2007, 2009). It is a multi-transmitter multi-receiver active electromagnetic system that is able to discriminate UXO from scrap at a single measurement position, hence eliminates a requirement of a very accurate sensor location. The cart-mounted system comprises of three orthogonal transmitters and eight pairs of differenced receivers (Smith et al., 2007). Receiver coils are located on symmetry lines through the center of the system and see identical fields during the on-time of the pulse in all of the transmitter coils. They can then be wired in opposition to produce zero output during the on–time of the pulses in three orthogonal transmitters. Moreover, this configuration dramatically reduces noise in the measurements by canceling the background electromagnetic fields (these fields are uniform over the scale of the receiver array and are consequently nulled by the differencing operation), and by canceling the noise contributed by the tilt of the receivers in the Earth's magnetic field, and therefore greatly enhances receivers sensitivity to the gradients of the target.

UXO detection and characterization (location, size, and symmetry properties of a suspected UXO) has been done by estimating the principal dipole polarizabilities of a target – a near intact UXO displays a single major polarizability coincident with the long axis of the object and two equal transverse polarizabilities, while scrap metal has three entirely different polarizabilities. This description of the inherent polarizabilities of a target is the key in

discriminating UXO from irregular scrap metal. Figures 1 and 2 illustrate a discrimination capability of the system for an UXO object (Figure 1), and scrap metal (Figure 2). While UXO objects have a single major polarizability coincident with the long axis of the object and two equal transverse polarizabilities (Figure 1), the scrap metal has three entirely different principal moments (Figure 2).

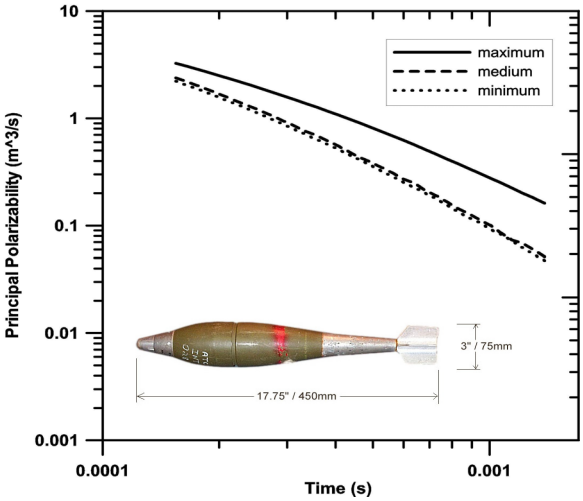

Figure 1. Inversion results for the principal polarizabilities of 81 mm mortar.

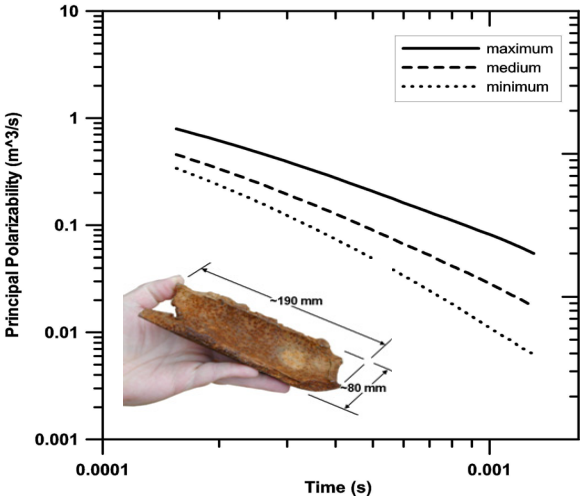

Figure 2. Inversion results for the principal polarizabilities of 19x8 cm scrap metal.

Hand-held systems have the advantage of being lightweight, portable, and deployable under most site conditions. They are particularly useful in areas of dense vegetation or challenging terrain, where lightweight and compact devices are required. In heavily wooded areas or areas with steep or uneven terrain, hand-held sensors may be the only suitable sensor deployment method. A useful criterion might be that it could be carried through spaces that the operator could walk through or at least approach. Further, it is desirable to find and characterize a metallic object without the need to accurately locate the sensors at multiple positions around the target. The ideal system would thus locate and characterize the target from a single position of the sensor and indicate to the operator where to flag the target for subsequent study.

2. Design and construction of a hand-held system

In a hand held system the sensor package must be easily maneuvered over rough terrain, through brush, etc. A useful criterion might be that it could be carried through spaces that the operator could walk through or at least approach. A major consideration is weight and the related size of the transmitter-receiver configuration. To a good approximation both signal-to-noise for a given transmitter moment (practically speaking, power) and size are proportional to the desired depth of detection/characterization of the UXO. Responses must be achieved over separations on the order of the depth and it is easily shown that the secondary field to be detected at a receiver from the UXO falls off very quickly ($1/\text{depth}^6$) as a fraction of the primary field at that receiver when the depth exceeds the size of the transmitter loop or the separation of the transmitter and receiver. Our modeling results and a preliminary structure design showed that we could achieve both of these goals with a 14-in (0.35 m) sensor cube.

To avoid the reliance on accurate multiple positioning of any system it has been shown that (1) the object must be illuminated with three different polarizabilities of transmitted field and that (2) to determine location from a single position of the transmitter-receiver system multiple spaced-apart receivers must be used. To accommodate the first requirement a hand-held design implements three orthogonal transmitter loops much like the cart-mounted system. To accommodate the second requirement the hand-held UXO identifier uses ten pairs of receivers. Any pair of receiver coils with identical frequency response that are placed symmetrically with respect to the cube center give no net

response to the primary magnetic field when their outputs are differenced. This cancels receiver voltages induced by the primary magnetic fields due to transmitter currents, leaving any measured response in differenced receiver pairs as due to induction in external objects. Given a finite accuracy in fabrication, the differencing of opposing receiver coils is expected to reduce the voltages induced by primary fields by a factor of 100 compared to voltages induced in the individual receiver coils.

2.1 System optimization and improvements

Our old proof-of-the-principle bench prototype of a hand-held UXO identifier had eight pairs of receivers (Figure 3a). We investigated improvements in resolution of closely spaced pairs of objects by a new hand-held UXO discriminator with addition of two or four receiver pairs. Addition of two receiver pairs (Figure 3b), allows resolution of principal polarizabilities of two 37 mm projectiles 0.4 m apart at 0.25 m depth from measurements at a single position of the system, suggesting better discrimination ability for closely spaced objects over the old system (Figure 4). Figures 4a and 4b show inversions results for the principal polarizabilities and locations of two 37 mm projectiles using data from eight and ten pairs of receivers, respectively. The inversion using data from eight pairs of receivers recovers correctly only one of the projectiles, while the inversion using data from ten pairs of receivers correctly identifies locations and responses of both projectiles. Addition of further two receiver pairs, to occupy every corner of every face of the UXO discriminator cube, marginally improves polarizability estimates for cases studied, although they will be very important if any of the channels malfunction in the field.

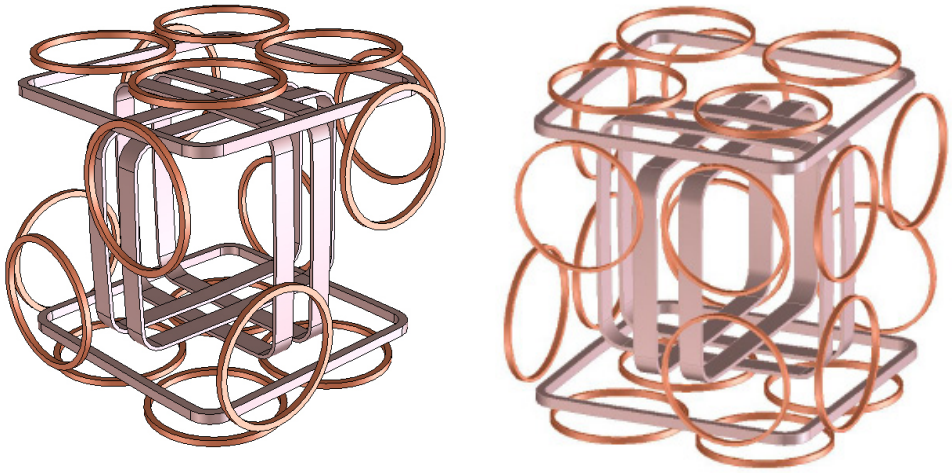

(a) (b)

Figure 3. Hand-held UXO discriminator – (a) old prototype, (b) new configuration.

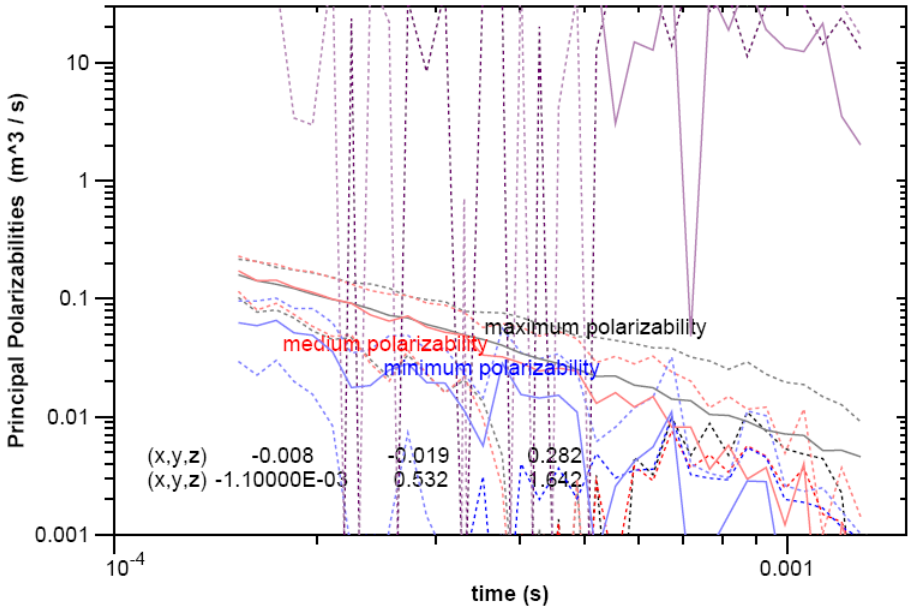

Figure 4a. Inversion results for the principal polarizabilities and locations of two 37 mm projectiles 0.4 m apart at 0.25 m depth using data from eight pairs of receivers.

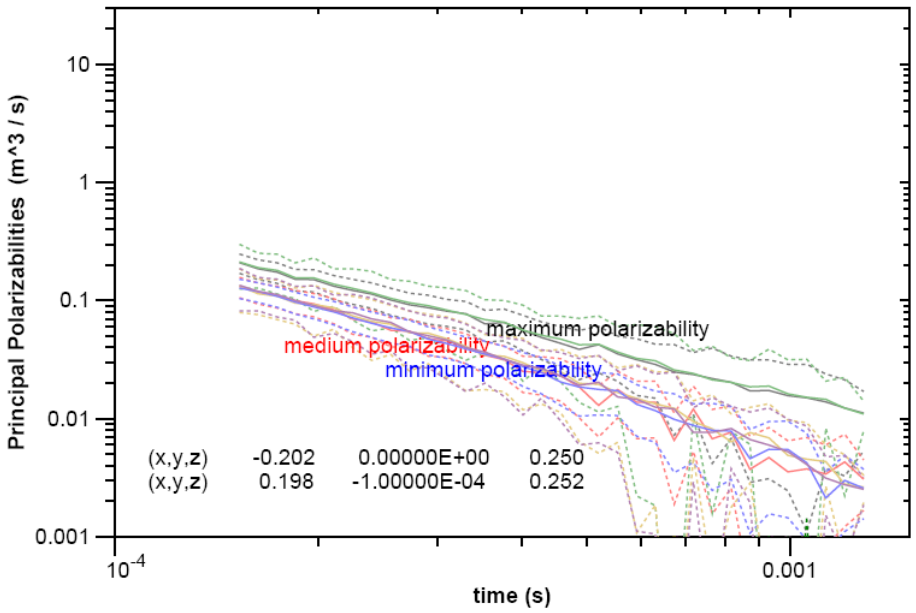

Figure 4b. Inversion results for the principal polarizabilities and locations of two 37 mm projectiles 0.4 m apart at 0.25 m depth using data from ten pairs of receivers.

We have investigated effect of a repetition rate, source pulse length, and receiver resonance frequency on uncertainty in ratio of spheroid conductivity to magnetic permeability (third best resolved parameter, after spheroid dimensions). Our results show a factor of four variation with respect to the receiver resonance frequency over range 5 kHz to 30 kHz, with a minimum near 20 kHz for a 20 mm x 80 mm steel spheroid (Figure 5a), and much less variation for 60 mm x 240mm steel spheroid with its minimum near 30 kHz (Figure 6a). Results also show a factor of six variation with the pulse length over the range 20 to 500 μs, with minimum near 300 μs for the 20 mm x 80 mm spheroid (Figure 5b), and near 420 μs for 60 mm x 240 mm spheroid (Figure 6b). Varying repetition rate over odd harmonics of 30 Hz from 270 to 690 Hz increases the uncertainty a factor of 10 from minimum at 270 Hz for both spheroids (Figure 5c and 6c).

Note, that increasing repetition rate shortens the length of interval of data collectible after the source pulse.

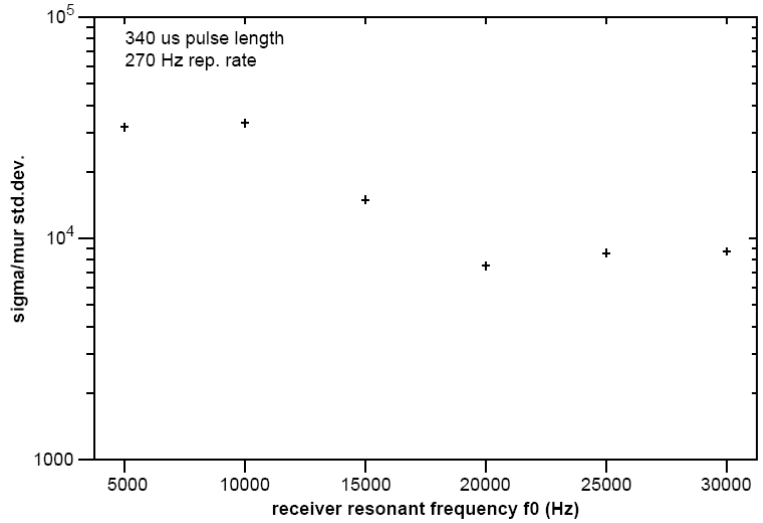

Figure 5a. Uncertainty in the ratio of spheroid conductivity to magnetic permeability as a function of receiver resonant frequency for 20x80 mm steel spheroid.

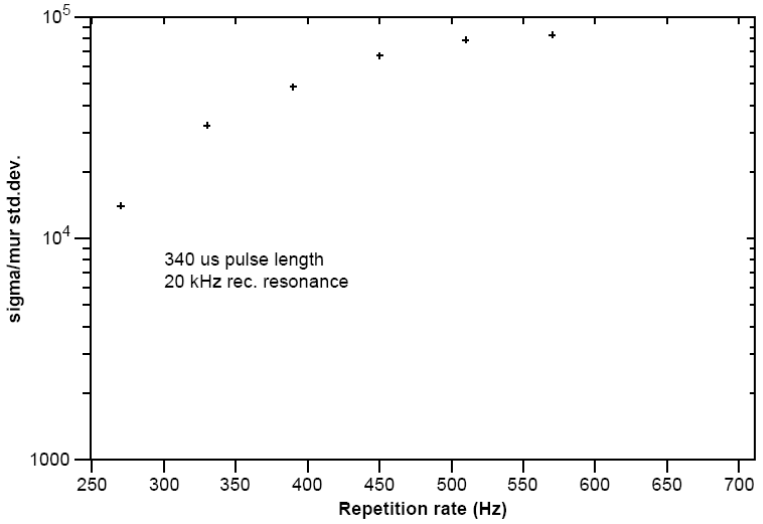

Figure 5b. Uncertainty in the ratio of spheroid conductivity to magnetic permeability as a function of a repetition rate for 20x80 mm steel spheroid.

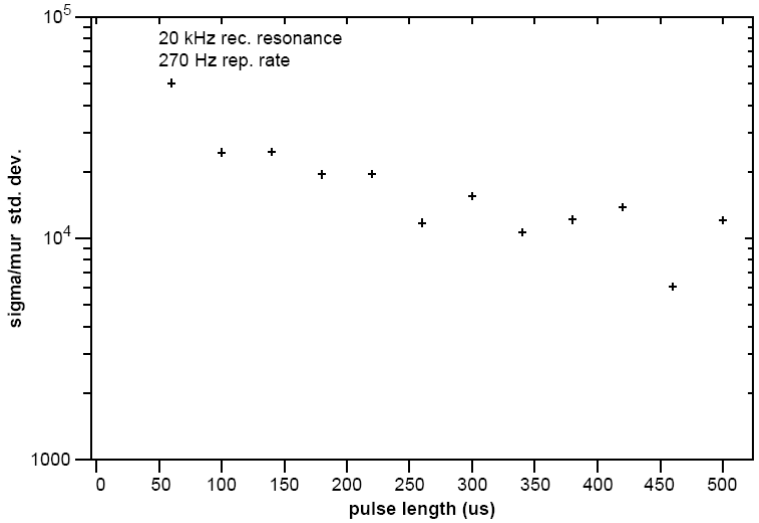

Figure 5c. Uncertainty in the ratio of spheroid conductivity to magnetic permeability as a function of a pulse length for 20x80 mm steel spheroid.

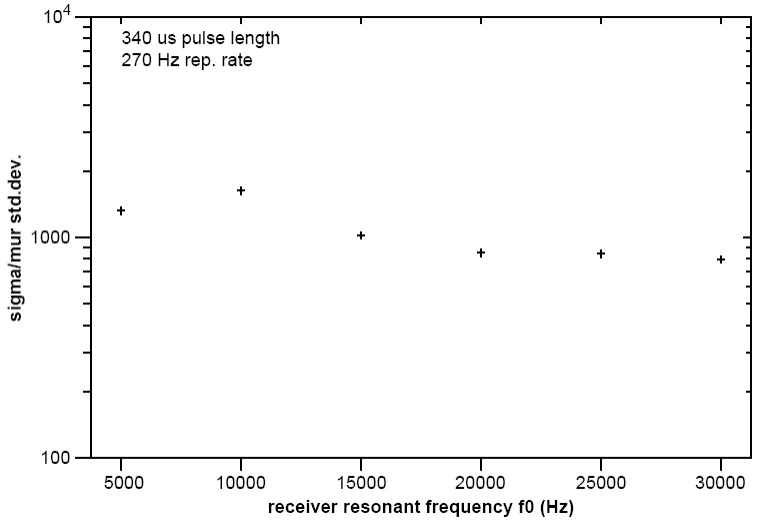

Figure 6a. Uncertainty in the ratio of spheroid conductivity to magnetic permeability as a function of receiver resonant frequency for 60x240 mm steel spheroid.

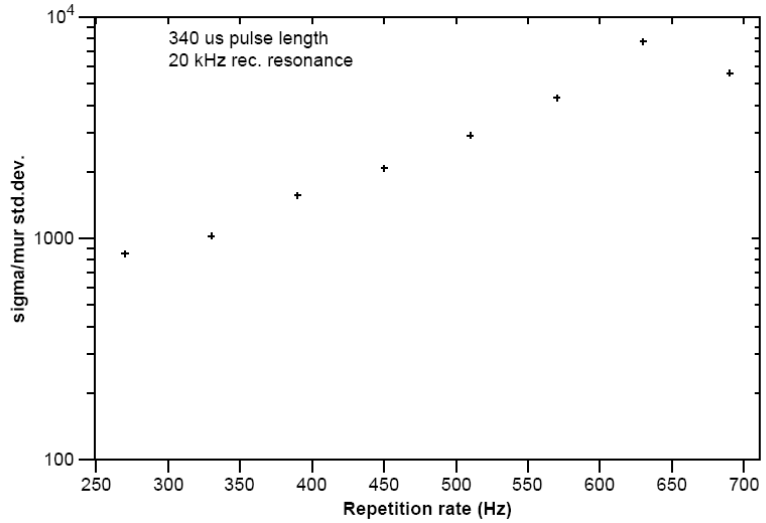

Figure 6b. Uncertainty in the ratio of spheroid conductivity to magnetic permeability as a function of a repetition rate for 60x240 mm steel spheroid.

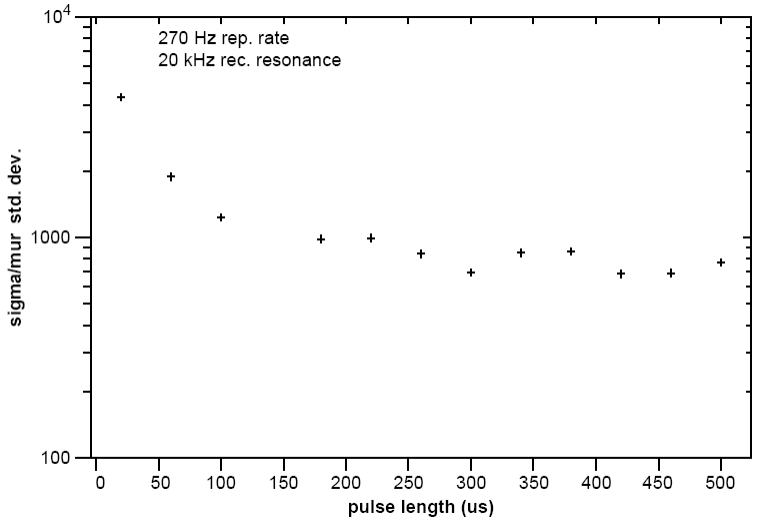

Figure 6c. Uncertainty in the ratio of spheroid conductivity to magnetic permeability as a function of a pulse length for 60x240 mm steel spheroid.

In order to facilitate the development of the system and its optimization, we wrote a new interface that allows us to operate the data acquisition system in a so-called oscilloscope mode. This makes the system a 10 channel, ultra high sensitivity device capable of

resolving voltages as small as 100 nV. The interface allows monitoring any or all of the 10 channels while energized by any of the three transmitters, so we can study each channel of the system in each plane. Additional features include memorizing a reference trace to compare with live channels, and stacking multiple traces by a variable amount of acquisitions.

2.2 System Description and Modeling

The overall system block diagram of Figure 7 shows how the FPGA contained in the digital board is at the center of the operation of the device. It is responsible for all functions, from distributing driver to the grounding of the system and its relation with transmitters and receivers, to minimize undesired noise. A local computer is connected via the USB 2.0 port to the FPGA logic board. Such computer is the local controller and not only configures the pulse timing and distributes triggers, but also collects all data through its USB link with the FPGA-based DAQ board. We developed a dedicated user interface that allows the expert user to rapidly setup and configure the system. The USB link has been successfully tested to transfer data at a speed of 33 MB/s, thus allowing for the direct transfer of data taken by all channels at 16-bit resolution when digitizing at the full 500 kS/s. Since the analog bandwidth is 40 kHz, the system is currently configured to run at 250 kS/s, resulting in a 8MB/s data transfer, although the board could support a higher transfer rate. The system can run in two modes of acquisition, one transferring raw data and one using FPGA stacked data only. In the latter mode, stacking of multiple data segments is performed on board; passing only the processed data to the local computer.

When the signal processing on the computer requires the complete data set, such as for noise spectrum measurements, stacking is disabled.

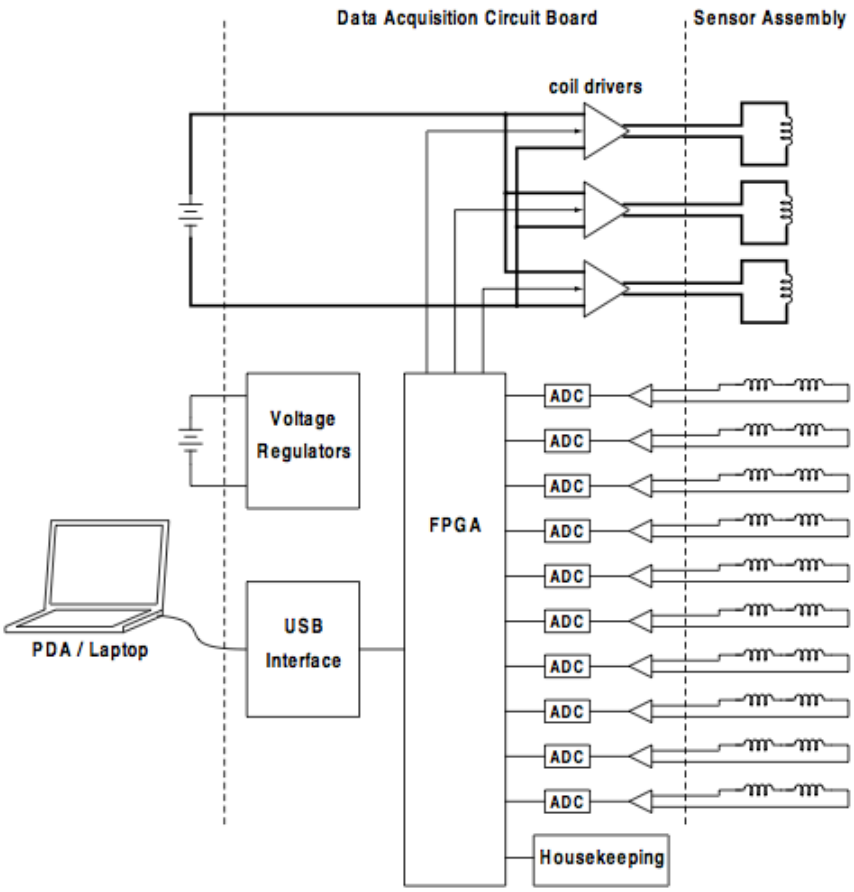

Figure 7. Block diagram of the hand-held UXO discriminator electronics.

A transmitter coil is driven by a pulser board to produce a half-sine bipolar excitation pulse. The analog front end of the transmitter circuit is triggered by a data acquisition (DAQ) board at the desired repetition rate. Pattern generation for controlling the triggering of transmitter coils and data collection is implemented inside the FPGA. All parameters of interest are adjustable, such as sampling rate, samples per cycle, pulse width, timing of gain switching, and pattern type. The receiver circuit consists of two

coils connected to a matching network with opposite polarities. The receivers can be connected in two configurations: (a) a parallel connection (T-termination mode), and (2) receivers are inverted and stacked (S-termination mode). The final design uses S-termination mode. Prior to analog to digital conversion (ADC), the signal measured by the receiver coils is amplified and filtered in order to limit noise bandwidth and aliasing. The output of the circuit is digitized and acquired by the FPGA.

We have used SPICE simulations to match the theoretical results to those from field experiments. The model has helped interpreting the data and identifying mismatches in the system. The parameter space investigated with these studies also included various capacitors, resistors, damping factors and coupling in both the S and T-termination modes. The accuracy of the model has been very satisfactory, as it has reproduced details observed in the field.

2.3 Component Studies

A study of components and subsystems included measuring the cube of the old prototype with eight pairs of receivers. Each receiver pair consisted of the so-called upper and lower coils that were terminated and connected to the respective channels on the DAQ board. The transmitter current was measured and connected to DAQ channel 9. The measurements showed an anomaly in pair#7 in which one coil showed a much higher resistance than any other coils. This has been verified in the original data taken when this cube was initially built and measured.

The study was aimed at identifying optimal materials to be used to build the components of a system. We also researched materials used in wires and wire insulation. As a result, we identified the preferred materials which to be used as follows: (1) teflon, (2) polypropylene, (3) polystyrene, (4) polyethylene (foam is better than solid).

2.4 Fabrication and assembly

The hand-held system is designed and generated by using a full 3D CAD system and modern fabrication techniques that allow for an easy, direct transfer of the drawings to the machine and a very quick turn around time. The core of the system is a foam block containing the groves for the transmitters in the X and Y planes and all mounting and alignment features to allow the full system integration. The system is made of two major subcomponents, the transmitter assembly and the receiver panels. All supporting electronics are assembled separately in a separate structure, made of wood and with plexiglass covers for personnel safety. The fabrication approach is modular, where all elements and built and stacked together.

The three transmitter coils (X, Y, and Z) in three orthogonal planes are made with coil pairs and wound with copper litz wire with Formvar insulation (Figure 8a). The sensors are 5-in critically damped coils (Figure 8b), with the respective resonant frequencies and time constants adjusted by the addition of adjustable external capacitances and resistances. The final choice of diameter, wire size, and number of turns was a compromise between sensitivity, self-resonance, internal resistance, and resolution. While a larger diameter results in a higher sensitivity, it also reduces resolution as the

signals are more distributed. Likewise, more turns offer a stronger signal, but lower the coil's self resonance which needs to remain above the desired operating band. The sensors are fabricated using a spool and wound using Formvar. After winding, we provide shielding using the copper etched method.

There are 12 possible pairs of receiver coils in the hand-held UXO discriminator, four per each plane (X, Y, and Z). Due to the limitation in readout channels in the DAQ board, the current system has ten pairs of receivers, with four pairs in the Z plane, and three pairs in the X and Y planes. This is consistent with our optimized design, which shows that ten receiver pairs guarantee improved discrimination capabilities. The coordinate system has been chosen such that Z is the vertical axis, pointing downwards, and the X and Y axis point as indicated in Figure 9. Particular care was given to shielding of the receiver and transmitter coils, to avoid or minimize the effects of transmitter pulses on the receivers and therefore improve our effective dynamic range. The electrostatic shielding is integrated into each receiver plate assembly by adding shield panels to each stack. Figures 8c and 8d show the modular assembly and assembled prototype, respectively.

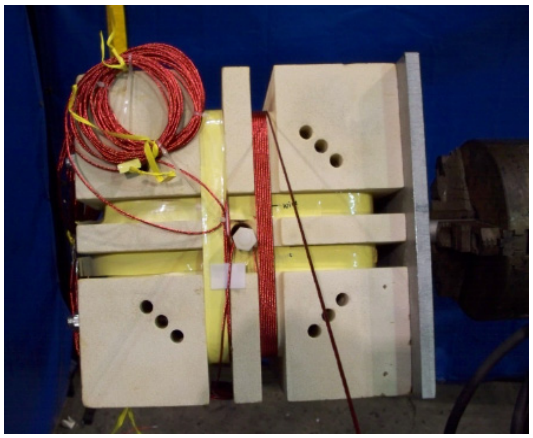

(a)

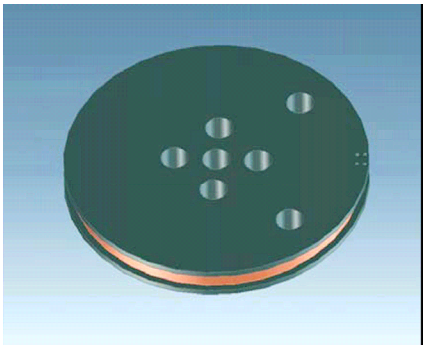

(b)

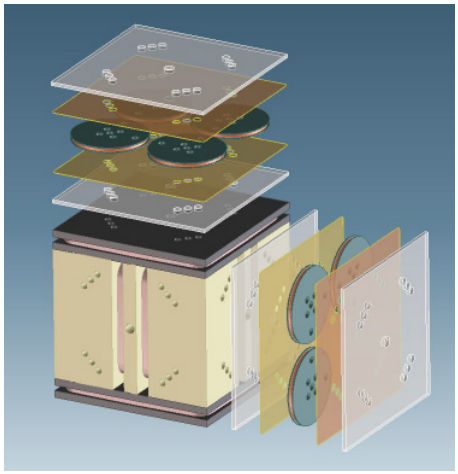

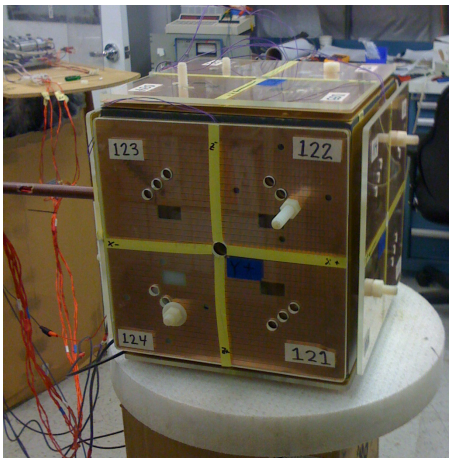

(c) (d)

Figure 8. Hand-held UXO discriminator – (a) transmitter coils winding, (b) receiver coil, (c) modular assembly, (d) assembled prototype.

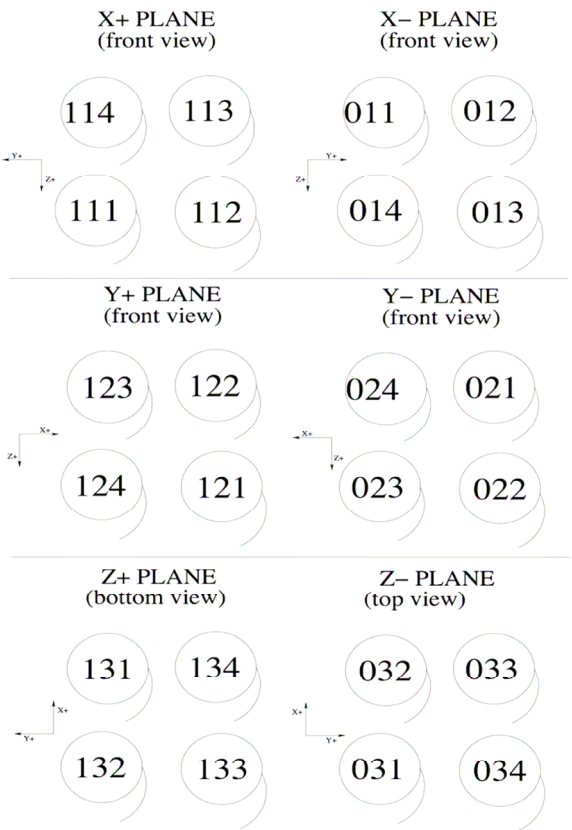

Figure 9. Hand-held receivers naming convention.

Single channel (one receiver pair) boards were built in both S and T-termination modes. One of the objectives was to reduce the spurious cable capacity by moving the preamplifier closer to the receivers and thus obtain a faster system. The other was to demonstrate the more promising feature of a 2.5 to 3 gain in the signal strength by adopting the S-termination. These boards were successfully measured but until now have not shown a significant increase in the system speed. While the final demonstration system was built without these boards, we are allowing for the implementation of such boards for improved performance.

3. Hand-held Simple System

Due to the great benefits we have had with the BUD cart by studying a much simplified configuration, we built a simple version of a hand-held cube, having only one transmitter and one receiver pair, the hand-held simple system (Figure 10), that can be easily reconfigured and tested. A support structure kit that was fabricated allows an easy addition of additional transmitters and/or receivers as needed. The hand-held simple system was used extensively to characterize the response of the system and to compare it with modeling efforts done in parallel. We started with 6-in receiver coils that were used in the cart-mounted system; once new 5-in coils were fabricated we used those in testing.

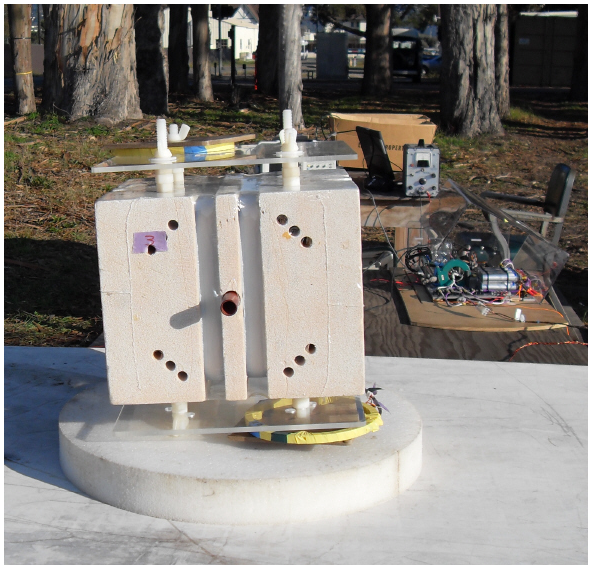

Figure 10. Hand-held simple system – one transmitter and one pair of receivers.

3.1 System Components Experiments

Intensive investigations were carried on the receiver parameters in order to match competing requirements on the rapidity of the response, which is inversely proportional to the coil inductance and would require a low number of turns, and the signal strength, governed by the coil area given by the coil diameter and number of turns. Similarly the distributed capacitance of the system contributes in slowing down its response, so we studied various ways to reduce that capacitance, starting from the winding of the receiver coils. The receiver coils that were built in different fashions were tested, and differences in the performance of these coils were observed, in order to select the final configuration. A self-supporting receiver coil is light but very delicate and requires careful handling. The performance between a receiver with a single groove and several spacers between layers of windings, and the one with triple groove and no spacers between layers of windings, on a teflon bobbin was only marginally different.

Starting from a single transmitter and a single unshielded receiver pair, the system was built up element by element up to two transmitter and three-shielded-coil pair system. We acquired data at each stage with the aim to analyze the system performance element by element. With one transmitter, a three-receiver pairs system could be well tuned and the receiver coil voltage decay was log linear and descended directly into the noise. Once the second transmitter was added, however, we were not able to obtain a similar result. Receivers were nearly well tuned but there was always at least one transmitter-receiver pair that exhibited an unwanted transient. The time at which the receiver decay entered the noise varied from around 450 μs to 600 μs. Our observations showed an extreme sensitivity of the system to an unbalanced termination circuit. The tuned system did not exhibit resonant frequency matching upper and lower coils in a pair; the difference up to 5 kHz between paired coils has been observed. Coils ring frequencies were most likely influenced by their mutual coupling to nearby coils.

Two new transmitter coils were fabricated for testing. Both these coils were circular, and of roughly the same area as our square coil. One of the new transmitters was wound with litz wire, and the other with our traditional solid aluminum wire. There was no significant difference in the response neither to the variation in shape, nor to the variation in wire material. We also collected some data with the toroid transmitter away from the receivers. In this case, the late transient was not observed. This also suggested that either coupling between the transmitter and other system components, or a strong primary field near the system, or both, caused the transient.

3.2 Shielding Experiments

The experiments were run at our field test site in Richmond, CA using the simple system that consisted of one transmitter and one pair of receivers. We experimented with coils using a variety of shielding configurations. These included unshielded, single-copper-wrap, single-aluminum-wrap, flat, double-flat with a spacer, and double-wrap-flat with spacers. Receiver coils used in our experiments up to this point have had single-copper-wrap type shields. Tape with copper coating on one side only was wrapped in a spiral pattern around the receiver coils in such a way that copper shields the whole receiver, but the shield did not form a closed loop. A closed loop here refers to loops having approximately the same radius and orientation as the receiver coil. The wrapping was done by hand, and thus there was some concern about the uniformity of the distributed capacitance from coil to coil. The distributed capacitance comes from the capacitance between overlapping layers of copper in the spiral as it is wound, from the fact that the shield sheaths back onto itself where it terminates, and finally because there is capacitance between the bulk shield and the receive coil itself. Aluminum-wrap shields were also hand made by wrapping an aluminum foil around the receiver coil, except for a small segment of the ring. Insulating tape was wrapped around the uncovered section as well as a couple inches of the foil adjacent to the uncovered section. Aluminum foil was then wrapped around the insulating tape so that it contacts with the previously wrapped aluminum on one side. The result was a coil completely shielded in aluminum, with no closed loops. Flat shields were made from the standard copper etchings, which we have been using on the cart-mounted system for the last several years. Flat shields were spaced by 1/8” to 1/16” cardboard or Plexiglas.

Wrapped shields were spaced by foam strips helically wrapped around the receive coil form. We experimented with grounding the shields several different ways as well. These included floating ground, grounded to the data acquisition board, grounded to 24 V capacitor, with permutations of grounding the shields individually using one wire for each shield, or joining the shields first at the coplanar array and running a single wire back to the designated ground. Our experiments demonstrated at least two reasons for grounded-shielded receivers - (1) they significantly reduce ambient noise, and (2) they allow more precise receiver tuning.

3.3 Ambient Background Measurements

Ambient background variations recorded with the transmitter off showed that the bucked receiver coils were an order of magnitude quieter than a lone shielded coil. The black curve in Figure 11 shows background variations (that's considered noise for our system) as a function of time for a differenced coil pair while the blue curve is for a single coil. The measurements were made for several hours in one-hour intervals, and the rms noise value for each sounding was calculated for each transmitter separately as shown in Figure 12 by different symbols. Figure 12a shows these noise values for the single coil, while Figure 12b illustrates the noise levels for the differenced-pair receiver.

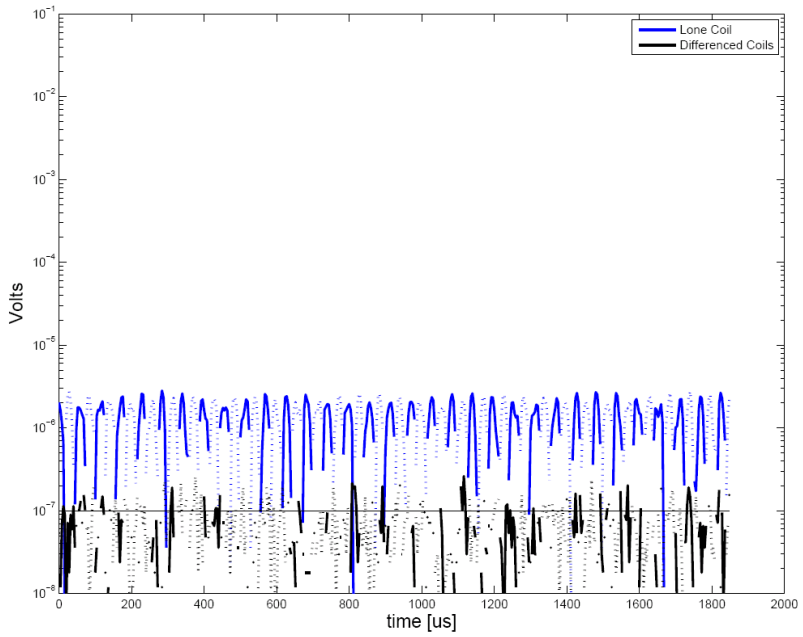

Figure 11. Ambient background variations (no transmitter) for a single coil (blue curve) and a differenced receiver pair (black curve) as a function of time.

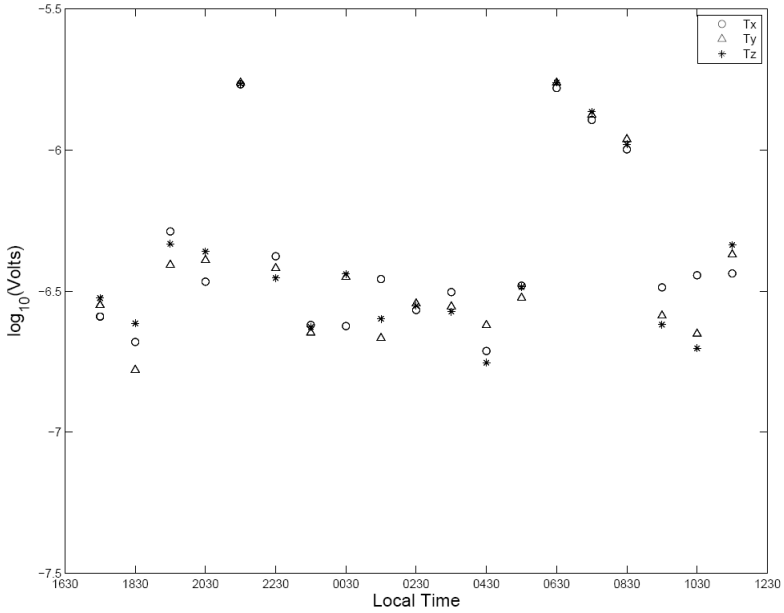

Figure 12a. RMS noise levels of ambient background variations (no transmitter) for a single coil.

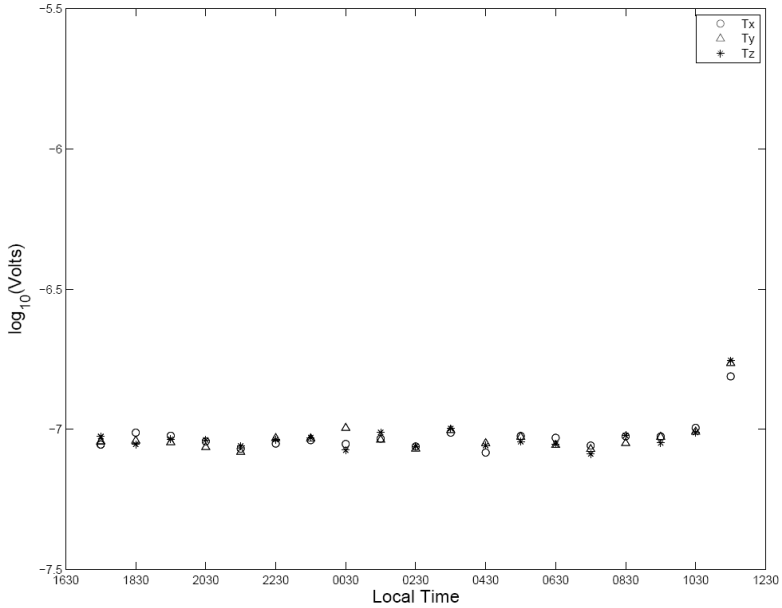

Figure 12b. RMS noise levels of ambient background variations (no transmitter) for a differenced pair receiver.

4. Conclusions

We have designed and built a sensor package of a 14-in (0.35 m) cube based on the considerations described in the Introduction. This hand-held prototype incorporates the key features of the cart-mounted system – (a) three orthogonal transmitters and ten pairs of receivers, and (b) difference or gradient measurements that significantly reduce the ambient and motion noise, and greatly enhance the sensitivity to the gradients of the target. We have also optimized the detector circuitry and improved electronics performance as well as many other system components. The next phase of this effort is to test the performance of the hand-held UXO discriminator prototype at a local test site.

5. Acknowledgments

This work was partially supported by the U.S. Department of Energy and LBNL under Contract No. DE-AC02-05CH11231, and the U. S. Department of Defense under the Strategic Environmental Research and Development Program Project MM-1667.

6. References

Baum, D., L. Doolittle, R. Lafever, M. Monroy, E. Norum, M. Placidi, A. Ratti, C. Serrano, V. Vytla, H. Yaver, 2010, BUD Hand Held, Technical Specification and System Design, LBNL Engineering Report.

Gasperikova, E., Smith, J.T., Morrison, H.F., and Becker, A., 2007, Berkeley UXO Discriminator (BUD): SAGEEP Proceedings, 1049–1055.

Gasperikova, E., Smith, J.T., Morrison, H.F., Becker, A., and Kappler, K, 2009, UXO detection and identification based on intrinsic target polarizabilities: Geophysics, 74, B1-B8.

Smith, J.T., and Morrison, H.F., 2004, Estimating equivalent dipole polarizabilities for the inductive response of isolated conductive bodies: IEEE Trans. Geosci. Remote Sensing, Vol. **42**, p. 1208-1214.

Smith, J.T., and Morrison, H.F., Becker, A., 2005, Optimizing receiver configurations for resolution of equivalent dipole polarizabilities in situ: IEEE Trans. Geosci. Remote Sensing, **43**, p. 1490 - 1498.

Smith, J.T., Morrison, H.F., Doolittle, L.R., and Tseng, H-W., 2007, Multi-transmitter null coupled systems for inductive detection and characterization of metallic objects: Journal of Applied Geophysics, **61**, 227–234.